Log-Domain Current-mode Quadrature Sinusoidal Oscillator

Pipat PROMMEE[1], *Nattawit PRAPAKORN*[1], *M. N. S. SWAMY*[2]

[1] Dept. of Telecommunication Engineering, Faculty of Engineering, King Mongkut's Institute of Technology Ladkrabang, Bangkok 10520, Thailand
[2] Dept. of Electrical and Computer Engineering, Faculty of Engineering and Computer Science, Concordia University, Montreal, Quebec, Canada

pipat@telecom.kmitl.ac.th

Abstract. *A log-domain current-mode quadrature sinusoidal oscillator based on lossless integrators is presented. The circuit is a direct realization of a first-order differential equation for obtaining the lossy and lossless integrators. Each of the log-domain lossless integrators is realized by using only NPN transistors and a grounded capacitor for achieving low-power and fast response. The proposed oscillator uses two-lossless integrator loop which can be electronically tuned through bias currents. A validated BJT model which is used in SPICE simulation operated from a single power supply as low as 2.5 V. The oscillation frequency is controlled over four decades of frequency. The total harmonic distortions for two-phases QSO (12 MHz) is obtained around 0.93% which enables fully integrated in telecommunication systems. The proposed circuit is also suitable for high-frequency applications. Nonideality studies are included and PSpice simulation results confirm the theoretical results.*

Keywords

Log-domain filtering, high-frequency, low-voltage, electronically-controlled, quadrature oscillator.

1. Introduction

In 1979, Adams introduced a novel class of continuous-time filters called log-domain filters which externally are linear systems, yet internally are nonlinear [1]. This class originates from the companding concept (compress and expand) of log-domain circuits. Input linear current is initially converted to a compressed voltage, which then is processed by the log-domain core block. The compressed output voltage is converted to a linear current to preserve the linear operation of the whole system. The compression and expansion of the corresponding signals are based on the logarithmic/exponential voltage–current relationship of a bipolar transistor. Log-domain circuits are useful building blocks for realizing high-performance current-mode analog signal processing systems.

In 1993, Frey introduced a general method for synthesizing log-domain filters of arbitrary order using a state-space approach [2], [3]. Frey also presented a highly modular technique for implementing such filters from a simple building block comprising a bipolar current mirror whose emitters are driven by complementary emitter followers. Log-domain filter operation is based on instantaneous companding [4]–[7] and these circuits are both of theoretical and technological interest, since they potentially offer high-frequency operation, tunability, and extended dynamic range under low power supply voltages [8]–[12].

Quadrature sinusoidal oscillator (QSO) is an oscillator that has two outputs with a 90 degree phase difference, and is useful in many applications. For example, in telecommunications QSO is used as phase modulator, quadrature mixer [13] and single-sideband generator [14]. For measurement purposes, QSO is used as a vector generator or a selective voltmeter [15]. Moreover, QSOs constitute an important unit in power electronics systems [16].

Several active building blocks, such as CF (current-follower) [17], OTA (operational transconductance amplifier) [18], FTFN (four terminal floating nullor) [19], FDCCII (fully-differential current conveyor) [20], CDTA (current differencing transconductance amplifier) [21] and DVCC (differential voltage current conveyor) [22] have been used for QSO realization. Some of them use floating passive elements [17], [18], [19], [21], [22], or excessive active components [20], or the frequency and condition of oscillation cannot be tuned independently [18]. Unfortunately, they are suitable only for low megahertz range.

This paper presents a new QSO realization based on a log-domain 2 lossless integrators loop. Fast response and low-power consumption are obtained. The proposed circuit possesses the following features:

- Simple structure which can be easily configured and realized by using the minimum number of active and passive components per phase.
- Use of grounded capacitors suitable for integration.
- A wide range electronic tunability of the oscillation frequency.

- High-frequency range of oscillation based on log-domain concept with electronic tunability and low-power supply feature.
- High-output impedance, thus allowing interconnection with succeeding current-mode circuits.

2. Theory and Principle

2.1 Quadrature Sinusoidal Oscillator

The generalized structure of a quadrature sinusoidal oscillator (QSO) is shown in Fig.1. It consists of inverting and non-inverting lossless integrators. The current output (I_o) of the second stage is fed back to the input of the first stage. The system is determined by the following transfer function.

$$H(s)=\frac{y(s)}{x(s)}=\left(-\frac{A}{s}\right)\left(\frac{kB}{s+B(1-k)}\right)=\frac{-kAB}{s^2+sA(1-k)}. \quad (1)$$

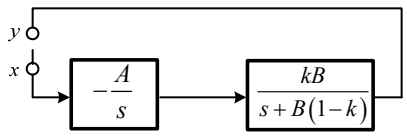

Fig. 1. Block diagram of QSO.

Rewriting (1) by using the Barkhausen's criteria yields

$$1-LG=0=\frac{N(s)}{D(s)}=1+\frac{kAB}{s^2+sA(1-k)}. \quad (2)$$

If $k = 1$, the numerator is given by

$$N(s)=0=s^2+AB. \quad (3)$$

It is seen that the frequency of oscillation is obtained by

$$\omega^2=AB. \quad (4)$$

2.2 Log-domain Lossless Integrator

Fig. 2(a) shows a log-domain filtering scheme based on a translinear type-B (balance) cell [23] which is called log-domain lossy integrator. Assuming that each transistor has an ideal exponential characteristic, and using Kirchhoff's current law (KCL), the base-emitter voltage relations can be written as

$$V_{be1}+V_{be2}-V_{be3}-V_{be4}=0. \quad (5)$$

The collector current of the transistor is given by

$$I_C=I_S\exp\left(\frac{V_{be}}{V_T}\right) \quad (6)$$

where the different terms have their usual meaning. Now, applying the translinear principle (TLP) [24] to Q_1-Q_4 gives

$$I_{C1}I_{C2}=I_{C3}I_{C4}. \quad (7.1)$$

If $I_{C1}= I_1$, $I_{C2}= I_{in}$ and $I_{C4}= I_{out}$, (7.1) becomes

$$I_1I_{in}=I_{C3}I_{out}. \quad (7.2)$$

The collector current of Q_3 can be expressed as

$$I_{C3}=I_3+C_1\dot{V}_{C1}. \quad (8)$$

The derivative of the voltage across the capacitor C_1 is

$$\dot{V}_{C1}=\frac{dV_{C1}}{dt}=\frac{V_T}{I_{out}}\frac{dI_{out}}{dt}=\frac{V_T\dot{I}_{out}}{I_{out}}. \quad (9)$$

The derivative of the output current based on (6) yields

$$\dot{I}_{out}=\frac{dI_{out}}{dt}=\frac{I_S}{V_T}\exp\left(\frac{V_{C1}}{V_T}\right)\frac{dV_{C1}}{dt}=\frac{I_{out}}{V_T}\dot{V}_{C1}. \quad (10)$$

Substituting (8), (9) and (10) into (7.2), we get

$$I_{in}I_1=\left(I_3+\frac{C_1\dot{I}_{out}V_T}{I_{out}}\right)I_{out}. \quad (11)$$

Suppose we define the currents $I_1= kI_3= kI$; then (11) becomes

$$kI_{in}=I_{out}+\frac{C_1\dot{I}_{out}V_T}{I}. \quad (12)$$

By taking the Laplace transform of both sides of (12) and rearranging, the transfer function of the circuit of Fig. 2(a) is given by

$$H(s)=\frac{I_{out}(s)}{I_{in}(s)}=\frac{k}{s(C_1V_T/I)+1} \quad (13)$$

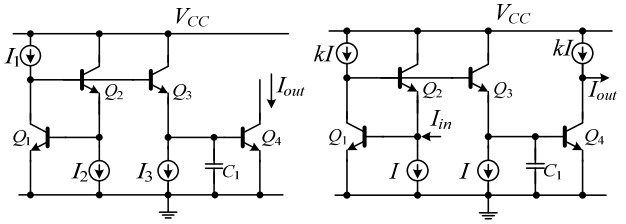

(a) (b)

Fig. 2. Log-domain lossy integrator.

From (13), where $k = I_1/I_3$, it is seen that $H(s)$ corresponds to the transfer function of a lossy integrator, and that the natural frequency is controlled by the bias current (I). Considering the direction of the input and output currents in Fig. 2(a) along with (13), it can be seen that this structure can easily produce a useful lossy integrator function. In Fig. 2(a), if the constant currents I_1, I_2, and I_3 are replaced by using $I_1= kI$, $I_2= I_3= I$, respectively, and current source kI is inserted at the output, then Fig. 2(a) is transformed to Fig. 2(b).

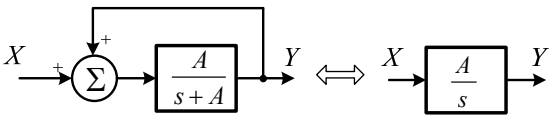

Fig. 3. Lossless integrator realized from lossy integrator.

Lossless and lossy integrators perform as dependent building blocks with the same frequency, but lossy integrator performs as a first order low-pass filter. Lossy integrator can be transformed by using lossless integrator and vice versa. This paper uses the transformation of a lossless integrator realized by using a lossy integrator. The non-inverting lossless integrators in Fig. 2 can be easily realized by positive feedback outputs.

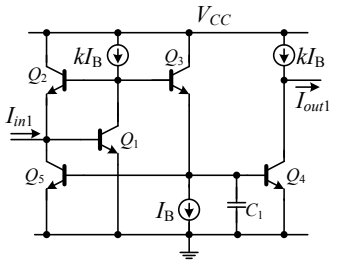

Fig. 4. Non-inverting log-domain lossless integrator realized by lossy integrator.

From Fig. 3 and Fig. 2(b), it is clear that a lossless integrator can be realized by positive feedback of the output I_{out} into the input by using a transistor Q_5. The complete non-inverting lossless integrator is depicted in Fig. 4 and its function is expressed by

$$\frac{I_{out1}(s)}{I_{in1}(s)} = \frac{\dfrac{kI_B}{C_1V_T}}{s + \dfrac{I_B}{C_1V_T}(1-k)} \tag{14}$$

Similarly, the inverting log-domain lossless integrator can be realized by adding the simple current mirror (inverting current amplifier) at the output. The completed inverting log-domain lossless integrator is shown in Fig.5. The identical bias current ($k = 1$) are applied then the function can be expressed as

$$\frac{I_{out2}(s)}{I_{in2}(s)} = -\frac{I_B}{sC_2V_T}. \tag{15}$$

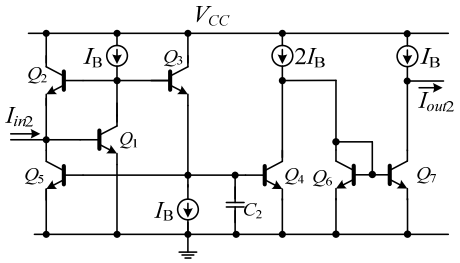

Fig. 5. Inverting log-domain lossless integrator realized by lossy integrator.

3. Current-mode Log-domain QSO

To confirm the theory, the quadrature sinusoidal oscillator based on the structure in Fig. 1 is implemented as shown in Fig. 6. Each integrator stage provides high output impedance that can drive the succeeding current-mode stage. The characteristic equation can be written as

$$s^2 + s\frac{I_B}{C_1V_T}(1-k) + \frac{k}{C_2C_1}\left(\frac{I_B}{V_T}\right)^2 = 0. \tag{16}$$

The condition of oscillation is obtained by setting $k = 1$ in (16). The frequency of oscillation (ω_0) can be expressed as

$$\omega_0 = \frac{I_B}{V_T\sqrt{C_1C_2}}. \tag{17}$$

The parameters I_B, and V_T represent controlled bias current and thermal voltage (≈26 mV at room temperature), respectively. From (17), ω_0 can be linearly tuned by adjusting biased current (I_B).

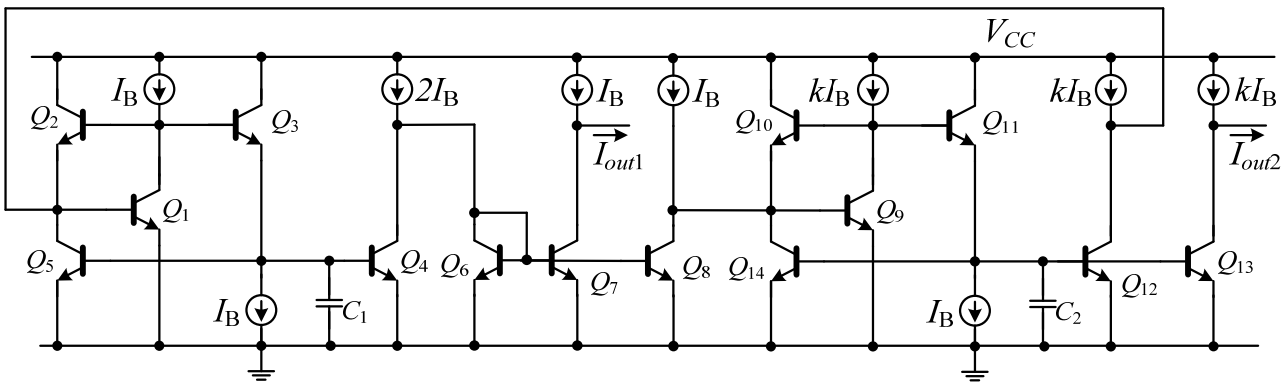

Fig. 6. Current-mode log-domain quadrature sinusoidal oscillator.

4. Nonideality Studies

Log-domain filter suffers from transistor nonidealities. The study of nonideal log-domain filters is complicated in view of the fact that the non-linear logarithmic-exponential operations inherent in the circuit result in transcendental equations. This paper derives equations describing the nonideal characteristics of log-domain circuit as a consequence of the deviations in the nonideal parameters. This section shows the effects of the transistor parasitic in Fig. 7 based on a small-signal model using base-emitter resistance (r_π), base-emitter capacitance (C_π), and base-collector capacitance (C_μ). We assume that the other parasitic capacitances are very small and the impedance of the collector-emitter (r_{ce}) is high. Physical parameters such as area mismatch and early voltage are also discussed.

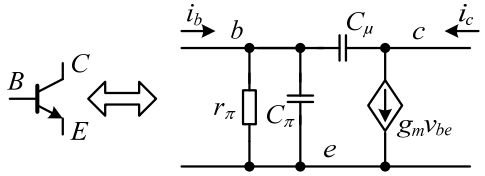

Fig. 7. Simple small signal of BJT transistor.

4.1 Parasitic Resistance (r_π and β)

Parasitic base-emitter resistance (r_π) is a major limitation of the translinear circuit accuracy at high-frequencies.

From the small-signal model of bipolar transistor, when the parasitic capacitances are neglected, the effect of r_π to non-inverting lossless integrator transfer function is described in (18). Assuming that the transconductances of the transistors are matched, the transfer function becomes (19.1).

Considering the transistor current gain $\beta_i = g_{mi} r_{\pi i}$, the frequency response of low-pass filter can be rewritten in terms of β as (19.2). From (19), it can be seen that the parasitic resistances and β produce a small deviation in the frequency response. The use of high current gain (β) transistors can reduce this effects.

4.2 Parasitic Capacitance (C_π and C_μ)

Parasitic base-emitter capacitance (C_π) is also a major limitation to translinear circuit accuracy, particularly at high-frequencies. Using the small-signal model of the bipolar transistor with parasitic capacitances, the effect of C_π to non-inverting lossless integrator transfer function can be approximated to (20). Again assuming that the transconductances of the transistors are matched, the transfer function becomes (21).

Similarly, parasitic base-collector capacitance (C_μ) is also a major limitation to translinear circuit accuracy. The effect of the base-collector capacitance to the non-inverting lossless integrator transfer function is given by (22). Assuming that the transconductances of the transistors are matched, the transfer function becomes (23).

$$\frac{i_{out1}(s)}{i_{in1}(s)} \approx \frac{g_{m4} r_{\pi4} r_{\pi5} \left(g_{m1} r_{\pi2} + g_{m1} g_{m3} r_{\pi2} r_{\pi3} - g_{m3} r_{\pi3} \right)}{\begin{aligned} &g_{m1} g_{m2} r_{\pi2} r_{\pi3} r_{\pi4} + g_{m1} g_{m3} r_{\pi3} r_{\pi4} r_{\pi5} + g_{m1} g_{m2} r_{\pi2} r_{\pi4} r_{\pi5} + g_{m1} g_{m2} g_{m3} r_{\pi2} r_{\pi3} r_{\pi4} r_{\pi5} \\ &+ g_{m1} g_{m2} r_{\pi2} r_{\pi3} r_{\pi5} + g_{m3} g_{m5} r_{\pi3} r_{\pi4} r_{\pi5} - g_{m1} g_{m5} r_{\pi2} r_{\pi4} r_{\pi5} - g_{m1} g_{m3} g_{m5} r_{\pi2} r_{\pi3} r_{\pi4} r_{\pi5} \\ &+ s\left(g_{m1} g_{m2} r_{\pi2} r_{\pi3} r_{\pi4} r_{\pi5} C_1 + g_{m1} r_{\pi3} r_{\pi4} r_{\pi5} C_1 + g_{m2} r_{\pi2} r_{\pi4} r_{\pi5} C_1 \right) \end{aligned}} \tag{18}$$

$$\frac{i_{out1}(s)}{i_{in1}(s)} \approx \frac{g_m r_{\pi4} r_{\pi5} \left(g_m r_{\pi2} r_{\pi3} + r_{\pi2} - r_{\pi3} \right)}{g_m r_{\pi3} \left(r_{\pi2} r_{\pi4} + 2 r_{\pi4} r_{\pi5} + r_{\pi2} r_{\pi5} \right) + s r_{\pi4} r_{\pi5} C_1 \left(g_m r_{\pi2} r_{\pi3} + r_{\pi2} + r_{\pi3} \right)} \tag{19.1}$$

$$\frac{i_{out1}(s)}{i_{in1}(s)} \approx \frac{\beta_4 r_{\pi5} \left(\beta_2 r_{\pi3} + r_{\pi2} - r_{\pi3} \right)}{\beta_3 \left(r_{\pi2} r_{\pi4} + 2 r_{\pi4} r_{\pi5} + r_{\pi2} r_{\pi5} \right) + s r_{\pi4} r_{\pi5} C_1 \left(\beta_2 r_{\pi3} + r_{\pi2} + r_{\pi3} \right)} \tag{19.2}$$

$$\frac{i_{out1}(s)}{i_{in1}(s)} \approx \frac{g_{m1} g_{m3} g_{m4} + s\left(g_{m1} g_{m4} C_{\pi3} - g_{m3} g_{m4} C_{\pi2} \right)}{g_{m1} g_{m2} g_{m3} - g_{m1} g_{m3} g_{m5} + s \begin{pmatrix} g_{m1} g_{m2} C_1 + g_{m1} g_{m2} C_{\pi3} + g_{m1} g_{m2} C_{\pi4} + g_{m1} g_{m2} C_{\pi5} \\ + g_{m1} g_{m3} C_{\pi2} + g_{m3} g_{m5} C_{\pi2} - g_{m1} g_{m5} C_{\pi3} \end{pmatrix}} \tag{20}$$

$$\frac{i_{out1}(s)}{i_{in1}(s)} \approx \frac{g_m}{s\left(C_1 + C_{\pi4} + C_{\pi5} + 2 C_{\pi2} \right)} \tag{21}$$

$$\frac{i_{out1}(s)}{i_{in1}(s)} \approx \frac{g_{m1} g_{m2} g_{m4} - s\left(g_{m3} g_{m4} C_{\mu1} + g_{m1} g_{m3} C_{\mu4} \right)}{g_{m1} g_{m2} g_{m3} - g_{m1} g_{m3} g_{m5} + s \begin{pmatrix} g_{m1} g_{m2} C_1 + g_{m1} g_{m2} C_{\mu5} + g_{m1} g_{m3} C_{\mu1} + g_{m2} g_{m3} C_{\mu2} \\ + g_{m3} g_{m5} C_{\mu1} + g_{m1} g_{m3} C_{\mu5} + g_{m2} g_{m3} C_{\mu3} + g_{m1} g_{m2} C_{\mu4} \end{pmatrix}} \tag{22}$$

$$\frac{i_{out1}(s)}{i_{in1}(s)} \approx \frac{g_m - s\left(C_{\mu 1} + C_{\mu 4}\right)}{s\left(C_1 + 2C_{\mu 1} + C_{\mu 2} + C_{\mu 3} + C_{\mu 4} + 2C_{\mu 5}\right)}. \quad (23)$$

From (21) and (23), it can be seen that parasitic capacitances $C_{\pi i}$ and $C_{\mu i}$ produce a small deviation in the frequency response of lossless integrators. This qualitative analysis shows that the transistor nonidealities, including the parasitic resistances and parasitic capacitances, are the sources of error within log-domain circuits. Finite beta and base-emitter resistance have generally been identified as the most problematic error sources at lower frequencies [25]. Since the natural frequency is of the form $\omega_0 = I / CV_T$, high frequency operation can be realized by increasing the bias current or by reducing the capacitance. To maintain the low-power, the bias currents are kept at a lower level and the integrating capacitance is increased. To prevent significant distortion, the selected capacitance C should be such that

$$C >> 4C_{\pi i} + 7C_{\mu i}. \quad (24)$$

Furthermore, equation (23) gives the zero, which affects the lossless integrators at very high frequencies. This zero can be approximately expressed as

$$z \approx \frac{g_m}{2C_{\mu i}}. \quad (25)$$

4.3 Area Mismatches

Emitter area mismatches cause variations in the saturation current (I_S) between transistors. Taking into account the emitter area, equation (12) can be rewritten as

$$\lambda k I_{in} = I_{out} + \frac{C_1 \dot{I}_{out} V_T}{I} \quad (26)$$

where $\lambda = \frac{I_{S3} I_{S4}}{I_{S1} I_{S2}} = \frac{A_3 A_4}{A_1 A_2}$.

From (26), it is clear that area mismatches introduce only a change in the proportionality constant or DC gain of the low-pass filter without affecting the linearity or the time constant of the circuit. The gain error can be easily compensated by adjusting one of the DC bias currents.

4.4 Early Effect

Early effect (base-width modulation) causes the collector current error by the collector-emitter and base-collector voltages. Considering the variation of collector-emitter voltage, the collector current can be written as $I_c = \left(1 + V_{ce}/V_A\right) I_S \exp\left(V_{be}/V_T\right)$, where V_A is the forward-biased early voltage. An analysis of the integrator shows the early effect with a scalar error to the DC gain of the circuit as in the case of area mismatches. Since V_{ce} is signal-dependent, the device base-width modulation also introduces distortion. Since the voltage swings in the current-mode companding circuits are very low ($\delta V_{be} s$), the early effect is not a major source of distortion.

4.5 Errors of Bias Currents

The proposed log-domain filter employs bias currents which are provided by positive and negative current sources. The positive (I_{BP}) and negative (I_{BN}) current sources are respectively replaced by positive and negative current mirrors in Fig. 8. The transconductance of transistors are controlled by the particular bias currents. Positive and negative current mirror errors which affect the filter performances are considered. Taking the small signal model into account, and neglecting the parasitic resistance and capacitance, the lossless integrator in Fig. 4 can be rewritten as

$$\frac{i_{out1}(s)}{i_{in1}(s)} = \frac{g_{m3} g_{m4} g_{m1}}{g_{m1} g_{m2} g_{m3} - g_{m1} g_{m3} g_{m5} + s\left(g_{m1} g_{m2} C_1\right)}. \quad (27)$$

Based on the configuration of Fig. 4, the positive and negative current biases are given by $I_{BP} = \alpha_P I_B$ and $I_{BN} = \alpha_N I_B$, where α_P and α_N represent the current gain of the positive and negative current mirrors, respectively. It can be seen that transconductances $g_{m2} = g_{m5}$, then equation (27) becomes

$$\frac{i_{out1}(s)}{i_{in1}(s)} = \frac{g_{m3} g_{m4}}{s g_{m2} C_1} = \frac{I_{BN} I_{BP}}{s V_T I_{BN} C_1} = \frac{\alpha_P I_B}{s V_T C_1}. \quad (28)$$

It can be seen that the current gain of current mirrors affect the translinear current gain and lossless integrator configuration. In view of this, the frequency of oscillation (ω_{0n}) can be rewritten as

$$\omega_{0n} = \frac{\alpha_P I_B}{V_T \sqrt{C_1 C_2}}. \quad (29)$$

As seen from (29) and (17), there is a slight deviation in the frequency of oscillation due to the mismatch in bias currents. The error of bias current can be eliminated by using the accurate bias currents as well as cascode current mirrors.

5. Simulation Results

In order to verify the operation of QSO topology in Fig. 6, power supply voltage is assigned to $V_{CC} = 2.5$ V, $k = 1.472$ and the bias current I_B was varied from 0.1 μA to 1,000 μA. To prevent the parasitic effects of the filter, capacitors should be much larger than $4C_\pi + 7C_\mu$ by assigning $C_1 = C_2 = 50$ pF. According to section 2, the low-frequency stage gain of lossless integrators must be unity based on identical current bias I_B. The NPN high-speed bipolar technology (HSB2) provided by ST Microelectronics [26] is used in the simulations and listed in Tab.

1(a). The bias currents realized by using the current mirrors as shown in Fig. 8 are provided by NPN and PNP (HFA3128 transistor arrays) models in Tab. 1(a) and (b), respectively. The two-phase current sinusoidal signal outputs are illustrated in Fig. 9. The simulated oscillation frequency is 12 MHz, while the theoretically predicted value is 12.24 MHz. Simulated values of power consumption are obtained around 2.46 mW. Two outputs are obtained 90 degree phase difference.

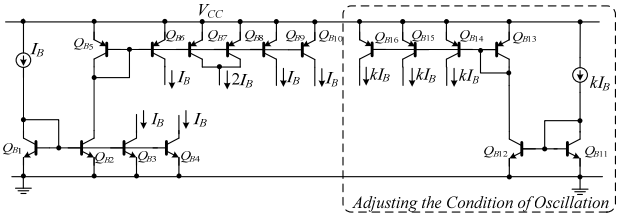

Fig. 8. Biasing circuit of proposed QSO.

(a) NPN-HSB2 provided by ST Microelectronics

```
.MODEL C12TYP NPN
+ (IS=7.40E-018 BF=1.00E+002 BR=1.00E+000 NF=1.00E+000
+ NR=1.00E+000 TF=6.00E-012 TR=1.00E-008 XTF=1.00E+001
+ VTF=1.50E+000 ITF=2.30E-002 PTF=3.75E+001 VAF=4.50E+001
+ VAR=3.00E+000 IKF=3.10E-002 IKR=3.80E-003 ISE=2.80E-016
+ NE=2.00E+000 ISC=1.50E-016 NC=1.50E+000 RE=5.26E+000
+ RB=5.58E+001 IRB=0.00E+000 RBM=1.55E+001 RC=8.09E+001
+ CJE=3.21E-014 VJE=1.05E+000 MJE=1.60E-001 CJC=2.37E-014
+ VJC=8.60E-001 MJC=3.40E-001 XCJC=2.30E-001 CJS=1.95E-014
+ VJS=8.20E-001 MJS=3.20E-001 EG=1.17E+000 XTB=1.70E+000
+ XTI=3.00E+000 KF=0.00E+000 AF=1.00E+000 FC=5.00E-001)
```

(b) PNP-HFA3128 provided by Intersil

```
.model HFA3128 PNP
+ (IS=1.027E-16 XTI=3.000E+00 EG=1.110E+00 VAF=3.000E+01
+ VAR=4.500E+00 BF=5.228E+01 ISE=9.398E-20 NE=1.400E+00
+ IKF=5.412E-02 XTB=0.000E+00 BR=7.000E+00 ISC=1.027E-14
+ NC=1.800E+00 IKR=5.412E-02 RC=3.420E+01 CJC=4.951E-13
+ MJC=3.000E-01 VJC=1.230E+00 FC=5.000E-01 CJE=2.927E-13
+ MJE=5.700E-01 VJE=8.800E-01 TR=4.000E-09 TF=20.05E-12
+ ITF=2.001E-02 XTF=1.534E+00 VTF=1.800E+00 PTF=0.000E+00
+ XCJC=9.000E-01 CJS=1.150E-13 VJS=7.500E-01 MJS=0.000E+00
+ RE=1.848E+00 RB=3
```

Tab. 1. Bipolar model parameter of used for SPICE simulation.

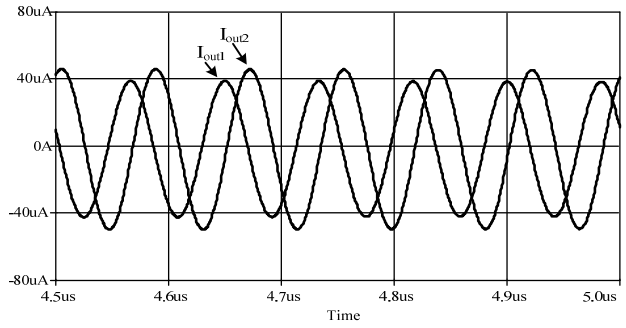

Fig. 9. Sinusoidal output 12 MHz when I_B= 100 μA.

The frequency spectrum of the sinusoidal signal output of Fig. 9 is shown in Fig. 10. The 2nd harmonic component is around 415.48 nA, while the amplitude of the fundamental component is around 43.57 μA; hence, the THD is around 0.93%.

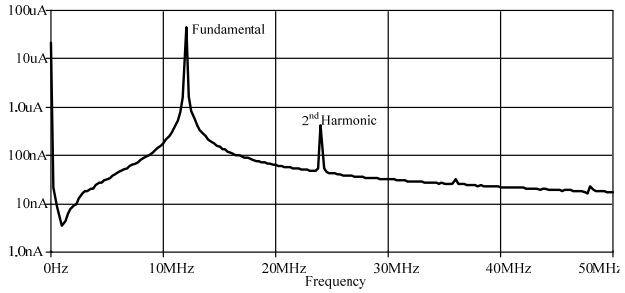

Fig. 10. Spectrum of signal in Fig. 8.

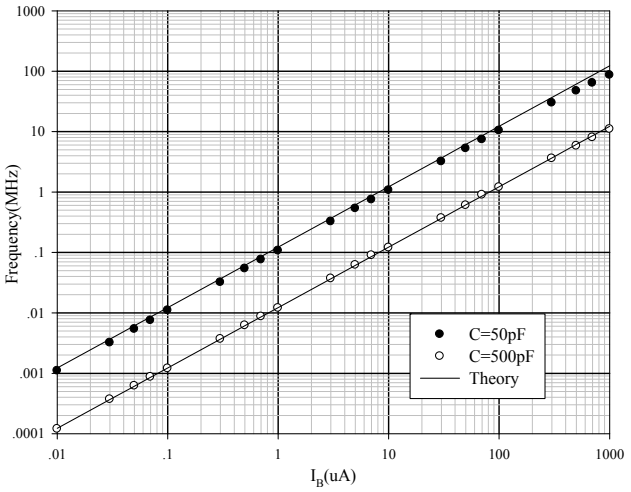

Fig. 11. Tunable frequency of oscillation by using various bias currents.

The tunable frequency of oscillation of QSO can be accommodated by varying the current bias (I_B) from 0.01 μA to 1,000 μA with different capacitor values. A comparison of the simulation and theoretical results are shown in Fig. 11. A wide-range of frequency of oscillation (from 1 kHz to 100 MHz) can be obtained based on C_1= C_2= 50 pF. The PSpice simulation results agree well with the theoretical results.

6. Conclusion

A novel low-voltage current-mode QSO based on log-domain lossless integrator has been presented. Lossless integrators are realized based on lossy integrator. Non-inverting lossless integrator is realized by five transistors and a grounded capacitor with three bias currents. Inverting lossless integrator is realized by seven transistors and a grounded capacitor with four bias currents. Inverting and non-inverting lossless integrator can easily be obtained based on the same configuration. This completed QSO consists of 14 transistors and 2 grounded capacitors with 9 bias currents. Quadrature output currents with high output impedance are produced based on a 2.5V power supply.

A wide-range of tunable frequency response (from 1 kHz to 100 MHz) can be obtained by varying I_B from 0.01 μA to 1,000 μA with a THD (12 MHz) around 0.93%.

References

[1] ADAMS, R. W. Filtering in the log domain. In *63rd AES Conf*., New York, N Y, 1979, preprint 1470.

[2] FREY, D. R. Log-domain filtering: An approach to current-mode filtering. *Proc. IEE, part-G*, 1993, vol. 140, no. 6, p. 406–416.

[3] FREY, D. R. Exponential state-space filters: a generic current mode design strategy. *IEEE Trans Circuits Systems-I*, 1996, vol. 43, p. 34–42.

[4] SEEVINCK, E. Companding current-mode integrator: A new circuit principle for continuous-time monolithic filters. *Electron. Lett*., 1990, vol. 26, no. 24, p. 2046–2047.

[5] TSIVIDIS, Y. On linear integrators and differentiators using instantaneous companding. *IEEE Trans. Circuits Syst. II*, 1995, vol. 42, p. 561–564.

[6] TSIVIDIS, Y. General approach to signal processors employing companding. *Electron. Lett*., 1995, vol. 31, no. 18, p. 1549–1550.

[7] TSIVIDIS, Y. Instantaneously companding integrators. In *Proc. IEEE Int. Symp. Circuits Syst. (ISCAS'97)*. Hong-Kong, 1997, vol. 1, p. 477–480.

[8] FREY, D. R. A 3.3 V electronically tunable active filter useable to beyond 1 GHz. In *Proc. IEEE Int. Symp. Circuits Syst. (ISCAS'94)*. London (U.K.), 1994, vol. 5, p. 493–496.

[9] FREY, D. R. Log domain filtering for RF applications. *IEEE J.Solid-State Circuits*, 1996, vol. 31, p. 1468–1475.

[10] FREY, D. R. An adaptive analog notch filter using log-filtering. In *Proc. IEEE Int. Symp. Circuits Syst. (ISCAS'96)*. Atlanta (GA), 1996, vol. 1, p. 297–300,.

[11] YANG, F., ENZ, C., RUYMBEKE, G. Design of low-power and low voltage log-domain filters. In *Proc. IEEE Int. Symp. Circuits Syst.(ISCAS'96)*. Atlanta (GA), 1996, vol. 1, p. 117–120.

[12] DRAKAKIS, E. M., PAYNE, A. J., TOUMAZOU, C. Log-domain filtering and the Bernoulli cell. *IEEE Trans. Circuits Syst. I*, 1999, vol. 46, no. 5, p. 559–571.

[13] DUNLOP, J., SMITH, D. G. *Telecommunications Engineering*. CRC Press, 3rd edition , Oct. 1994.

[14] TOMASI, W. *Electronic Communications Systems*. New Jersey: Prentice-Hall Inc., 1988.

[15] ANRITSU EMEA LIMITED: MG3700A vector signal generator datasheet, Available at: http://www.eu.anritsu.com/files/MG3700A_ EI7301.pdf.

[16] EIREA, G., SANDERS, S. R. Phase current unbalance estimation in multiphase buck converters. *IEEE Trans. Power Elect.,* 2008, vol. 23, no. 1, p. 137-143.

[17] ABUELMA'ATTI, M. T. Grounded capacitor current-mode oscillator using single current follower. *IEEE Transactions on Circuits and Systems-I*, 1992, vol. 39, p. 1018-1020.

[18] AHMED, M. T., KHAN, I. A., MINHAJ, N. On transconductance-C quadrature oscillators. *Int. J. Electron.,* 1997, vol. 83, p. 201-207.

[19] LIU, S. I. LIAO, Y. H. Current-mode quadrature sinusoidal oscillatorusing single FTFN. *Int. J. Electron.,* 1996, vol. 81, p. 171-175.

[20] HORNG, J. W., HOU, C. L., CHANG, C. M., CHOU, H. P., WEN, Y. H. Quadrature oscillator with grounded capacitors and resistors using FDCCIIs. *ETRI Journal*, 2006, vol. 28, p. 486-494.

[21] KESKIN, A. U., BIOLEK, D. Current-mode quadrature oscillator using current differencing transconductance amplifier (CDTA). *IEE Proceeding of Circuits Devices and Systems*, 2006, vol. 153, p. 214-218.

[22] HORNG, J. W. Current-mode quadrature oscillator with grounded capacitors and resistors using two DVCCs. *IEICE Transaction on Fundamentals of Electronics, Communications and Computer Sciences*, 2003, vol. E86-A, p. 2152-2154.

[23] TOUMAZOU, C., LIDGEY, F. J., HAIGH, D. G. *Analog IC Design: The Current-Mode Approach*. London: Peter Peregrinus Ltd., 1990.

[24] GILBERT, B. Translinear circuits: an historical overview. *Analog Integrated Circuits and Signal Processing,* 1996. vol. 9, no. 2, p. 95-118.

[25] LEUNG, V. W., ROBERTS, G. W. Effects of transistor nonidealities on high-order log-domain ladder filter frequency responses. *IEEE Trans. Circuits Syst. II*, 2000, vol. 47, no. 5, p. 373-387.

[26] ALIOTO, M., PALUMBO, C. *Model and Design of Bipolar and MOS Current-Mode Logic: CML, ECL and SCL Digital Circuits*. Dordrecht, Netherlands: Springer, 2005.

About Authors

Pipat PROMMEE received his B. Ind. Tech. degree in Telecommunications, M. Eng. and D. Eng. in Electrical Engineering from the Faculty of Engineering, King Mongkut's Institute of Technology Ladkrabang (KMITL), Bangkok, Thailand in 1992, 1995 and 2002, respectively. He was a senior engineer of CAT telecom plc. between 1992 and 2003. Since 2003, he has been a faculty member of KMITL. He is currently an assistant professor at telecommunications engineering department at KMITL. His research interests are focusing in Analog Signal Processing, Analog Filter Design and CMOS Analog Integrated Circuit Design. He is a member of IEEE, USA.

Nattawit PRAPAKORN received B.Eng. and M.Eng. degrees in Telecommunications Engineering from the Faculty of Engineering, King Mongkut's Institute of Technology Ladkrabang (KMITL), Bangkok, Thailand in 2006, and 2008, respectively. He was a telecommunications engineer of AIN GlobalComm Co., Ltd since 2006-2008, and Ericsson Egypt Ltd. as a professional consultant between 2008 and 2009. He is presently working toward his D.Eng. in Electrical Engineering at KMITL. His research interests are focusing in analog filter design and analog signal processing.

M. N. S. SWAMY received the B.Sc. (Hons.) degree in Mathematics from Mysore University, Mysore, India, in 1954, D.I.I.Sc. (Diploma of the Indian Institute of Science, Bangalore, India) in Electrical Communication Engineering, in 1957, and the M.S. and Ph.D. degrees in Electrical Engineering from the University of Saskatchewan, Saskatoon, Canada, in 1960 and 1963, respectively. In August

2001, he was awarded the Doctor of Science (Honoris Causa) degree in engineering by Ansted University, Malaysia. He is currently a Research Professor in the Department of Electrical and Computer Engineering, Concordia University, Montreal, Quebec, Canada, where he has served as the Founding Chair of the Department of Electrical Engineering from 1970 to 1977, and the Dean of Engineering and Computer Science from 1977 to 1993. During that time he developed the faculty into a research oriented faculty from what was primarily an undergraduate one. Since 2001, he holds the Concordia University Research Chair (Tier I) in Signal Processing. He has also taught in the Department of Electrical Engineering, Technical University of Nova Scotia, Halifax, and the University of Calgary, Calgary, as well as in the Department of Mathematics, University of Saskatchewan. He has published extensively in the areas of number theory, circuits, systems and signal processing, and holds five patents. One of the books, Graphs, Networks and Algorithms (New York: Wiley, 1981), has been translated into Russian (Moscow, Russia: Mir, 1984) and Chinese (Beijing, China: Education Press, 1987).

Dr. Swamy is a Fellow of a number of professional societies, including the Institute of Electrical and Electronic Engineers, Institute of Electrical Engineers, U. K., the Engineering Institute of Canada, the Institution of Engineers, India, and the Institution of Electronic and Telecommunication Engineers, India. He was a Founding Member of Micronet from its inception in 1999 as a Canadian Network of Centers of Excellence until its expiration in 2004, and also its coordinator for Concordia University. In 2008, Concordia University has instituted the M. N. S. Swamy Research Chair in Electrical Engineering as a recognition of his research contributions. He was conferred in 2009, the title of Honorary Professor at the National Chiao Tung University in Taiwan. He has served the IEEE in various capacities such as the President-Elect in 2003, the President in 2004, the Past-President in 2005, the Vice President (Publications) from 2001 to 2002, the Vice-President in 1976, the Editor-in-Chief of the IEEE Transactions on Circuits and Systems-I from 1999 to 2001, the Associate Editor of the IEEE Transactions on Circuits and Systems from 1985 to 1987, the Program Chair for the 1973 IEEE Circuits and Systems (CAS) Symposium, the General Chair for the 1984 IEEE CAS Symposium, the Vice-Chair for the 1999 IEEE CAS Symposium, and a Member of the Board of Governors of the CAS Society. He is the recipient of many IEEE-CAS Society Awards, including the Education Award in 2000, the Golden Jubilee Medal in 2000, and the 1986 Guillemin–Cauer Best Paper Award.